

# Present-Day Star Formation: Protostellar Outflows and Clustered Star Formation

Fumitaka Nakamura\* and Zhi-Yun Li†

*\*National Astronomical Observatory of Japan; Mitaka, Tokyo 181-8588, Japan;  
fumitaka.nakamura@nao.ac.jp*

*†Department of Astronomy, University of Virginia, P.O. Box 400325, Charlottesville, VA 22904,  
USA; z14h@virginia.edu*

**Abstract.** Stars form predominantly in clusters inside dense clumps of turbulent, magnetized molecular clouds. The typical size and mass of the cluster-forming clumps are  $\sim 1$  pc and  $\sim 10^2 - 10^3 M_\odot$ , respectively. Here, we discuss some recent progress on theoretical and observational studies of clustered star formation in such parsec-scale clumps with emphasis on the role of protostellar outflow feedback. Recent simulations indicate that protostellar outflow feedback can maintain supersonic turbulence in a cluster-forming clump, and the clump can keep a virial equilibrium long after the initial turbulence has decayed away. In the clumps, star formation proceeds relatively slowly; it continues for at least several global free-fall times of the parent dense clump ( $t_{\text{ff}} \sim \text{a few} \times 10^5$  yr). The most massive star in the clump is formed at the bottom of the clump gravitational potential well at later times through the filamentary mass accretion streams that are broken up by the outflows from low-mass cluster members. Observations of molecular outflows in nearby cluster-forming clumps appear to support the outflow-regulated cluster formation model.

**Keywords:** ISM: clouds, ISM: jets and outflows, ISM: magnetic fields, MHD, stars: formation, turbulence

**PACS:** 97.10.Bt

## INTRODUCTION

Most stars form in clusters (Lada & Lada 2003). Therefore, understanding the formation process of star clusters is a key step towards a full understanding of how stars form. Recent observations have revealed that star clusters form in turbulent, magnetized, parsec-scale dense clumps of molecular clouds (Ridge et al. 2003). These clumps contain masses of  $10^2 - 10^3 M_\odot$ , fragmenting into an assembly of cores that collapse to produce stars. In cluster-forming clumps, stellar feedback such as protostellar outflows, stellar winds, and radiation rapidly start to shape the surroundings. Because of the short separations between forming stars and cores, these feedback mechanisms are expected to control subsequent star formation.

Among the stellar feedback processes, protostellar outflow feedback has been considered to be one of the important mechanisms that control the structure and dynamical properties of cluster-forming clumps (e.g., Matzner & McKee 2000) because the outflows from a group of young stars interact with a substantial volume of their parent clump by sweeping up the gas into shells. Furthermore, in nearby cluster-forming clumps which are forming no massive stars that would emit strong UV radiation, the protostellar outflow feedback is considered to be the dominant feedback mechanism. Recent numerical simulations of cluster formation have demonstrated that the proto-

stellar outflows largely regulate the structure formation and star formation in a dense cluster-forming clump. Li & Nakamura (2006) showed that the supersonic turbulence in dense clumps can be maintained by the momentum injection from the protostellar outflows (see also Carroll et al. 2009). The moderately-strong magnetic fields are also important to impede the rapid global gravitational collapse. In this case, the global inflow and outflow are expected to coexist, interacting with themselves. As a result, the cluster-forming clumps as a whole can keep quasi-equilibrium states for a relatively long time. Furthermore, Nakamura & Li (2007) showed that the global star formation efficiency tends to be reduced by the momentum injection from the protostellar outflows, although local star formation can often be triggered by the dynamical compression due to the protostellar outflows.

In this contribution, we discuss several important characteristics of this outflow-regulated cluster formation model and compare the theoretical model with observations of nearby cluster-forming regions.

## **OUTFLOW-REGULATED CLUSTER FORMATION**

Most, perhaps all, stars go through a phase of vigorous outflow during formation. Li & Nakamura (2006) examined, through 3D MHD simulation, the effects of protostellar outflows on cluster formation. They found that the initial turbulence in the cluster-forming region is quickly replaced by motions generated by outflows. The protostellar outflow-driven turbulence (“protostellar turbulence” for short) can keep the region close to a virial equilibrium long after the initial turbulence has decayed away. Therefore, there exist two types of turbulence in star-forming clouds: a primordial (or “interstellar”) turbulence and a protostellar turbulence, with the former transformed into the latter mostly in embedded clusters such as NGC 1333. Collimated outflows are more efficient in driving turbulence than spherical outflows that carry the same amounts of momentum. This is because collimated outflows can propagate farther away from their sources, effectively increasing the turbulence driving length; turbulence driven on a larger scale decays more slowly. Gravity plays an important role in shaping the turbulence, generating infall motions that balance the outward motions driven by outflows. Since the majority of stars are thought to form in clusters, an implication is that the stellar initial mass function is determined to a large extent by the stars themselves, through outflows that individually limit the mass accretion onto forming stars and collectively shape the environments (density structure and velocity field) in which most cluster members form. Thus, massive cluster-forming clumps supported by protostellar turbulence gradually evolve toward a highly centrally condensed “pivotal” state, culminating in rapid formation of massive stars in the densest part through accretion (see below for massive star formation). Here, we call this cluster formation scenario “outflow-regulated cluster formation”.

### **Star Formation Rate in Cluster Formation**

Using 3D MHD numerical simulations of cluster formation, Li & Nakamura (2006) and Nakamura & Li (2007) demonstrated that the protostellar outflow-driven turbulence

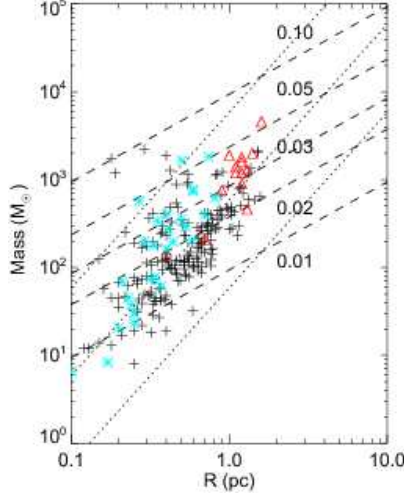


**FIGURE 1.** Contours of  $\text{SFR}_{\text{ff}}$  predicted by the outflow-regulated cluster formation model on the mass-radius diagram. The dashed contours are labeled by values of  $\text{SFR}_{\text{ff}}$ . The dotted contours indicate the constant column density at  $10^{21} \text{ cm}^{-2}$  (*bottom line*),  $10^{22}$  (*intermediate line*), and  $10^{23} \text{ cm}^{-2}$  (*upper line*). The crosses and triangles indicate the cluster-forming clumps identified by Ridge et al. (2003) and Higuchi et al. (2009), respectively. The asterisks indicate the dense clumps in the IRDCs identified by Rathborne et al. (2006). For most of the dense clumps, the predicted  $\text{SFR}_{\text{ff}}$  ranges from 1 % to 5 %. See Nakamura & Li (2011) in more detail.

can keep a pc-scale, cluster-forming clump close to a virial equilibrium long after the initial turbulence has decayed away. Here, we derive an analytic formula of star formation rate in a cluster-forming clump that keeps its virial equilibrium by the protostellar outflow feedback.

Numerical simulations of protostellar turbulence indicate that the dissipation rate of the turbulence momentum,  $dP_{\text{turb}}/dt$ , balances the momentum injection rate by the protostellar outflow feedback,  $dP_{\text{out}}/dt$ , so that the clump can be kept close to a virial equilibrium. Adopting the virial equilibrium condition, Nakamura & Li (2011) derived the predicted star formation rate per free-fall time ( $\text{SFR}_{\text{ff}}$ ) toward observed cluster-forming clumps as follows.

$$\text{SFR}_{\text{ff}} \simeq 0.0125\alpha \left(\frac{f_{\text{B}}}{0.5}\right) \left(\frac{f_{\text{w}}}{0.5}\right)^{-1} \left(\frac{V_{\text{w}}}{10^2 \text{ km s}^{-1}}\right)^{-1} \left(\frac{R_{\text{cl}}}{1 \text{ pc}}\right)^{1/2} \left(\frac{\Sigma_{\text{cl}}}{5 \times 10^{21} \text{ cm}^{-2}}\right)^{1/2}. \quad (1)$$

Figure 1 shows the dependence of  $\text{SFR}_{\text{ff}}$  on the mass and radius. The outflow-regulated cluster formation model suggests that the star formation rate per free-fall time ranges from 1 % to 5 % for the observed cluster-forming clumps in the solar neighborhood when the protostellar outflow feedback maintains the supersonic turbulence in the clumps, indicating that it takes about  $(2 - 10) t_{\text{ff}}$  for the star formation efficiency to reach about  $(10 - 20) \%$ .

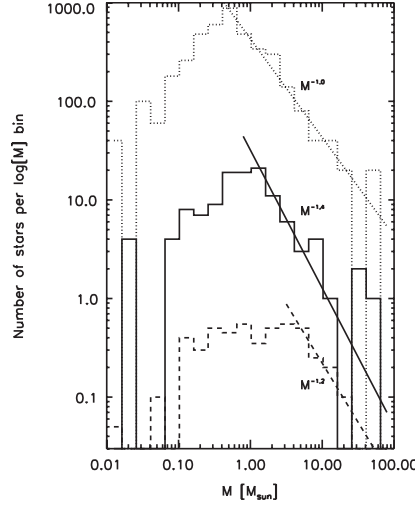


**FIGURE 2.** Power-law fits to the high mass end of the stellar mass distributions of the three models: HD (without outflow and magnetic field, dashed lines), MHD (without outflow, solid), and WIND (with outflow and magnetic field, dotted). The top (bottom) curve is raised (lowered) by a factor of 20 for clarity. See Li et al. (2010) in more detail.

## Massive Star Formation

In the outflow-regulated cluster formation, massive stars are predicted to form in later phases of cluster formation at the bottom of the global gravitational potential, or at the central densest part. Wang et al. (2010) investigated massive star formation in turbulent, magnetized, parsec-scale clumps of molecular clouds including protostellar outflow feedback using 3D numerical simulations of effective resolution  $2048^3$ . The calculations are carried out using a block structured adaptive mesh refinement code, ENZO, that solves the ideal magnetohydrodynamic equations including self-gravity and implements accreting sink particles. They found that, in the absence of regulation by magnetic fields and outflow feedback, massive stars form readily in a turbulent, moderately condensed clump of about  $1600M_{\odot}$  (containing about 100 initial Jeans masses), along with a cluster of hundreds of lower mass stars. The massive stars are fed at high rates by (1) transient dense filaments produced by large-scale turbulent compression at early times and (2) by the clump-wide global collapse resulting from turbulence decay at late times (see also Smith et al. 2009). In both cases, the bulk of the massive star’s mass is supplied from outside a 0.1 pc-sized core that surrounds the star. In the simulation, the massive star is clump-fed rather than core-fed. The need for large-scale feeding makes the massive star formation prone to regulation by outflow feedback, which directly opposes the feeding processes. The outflows reduce the mass accretion rates onto the massive stars by breaking up the dense filaments that feed the massive star formation at early times, and by collectively slowing down the global collapse that fuels the massive star formation at late times. The latter is aided by a moderate magnetic field of strength in the observed range (corresponding to a dimensionless clump mass-to-flux ratio  $\sim$  a few); the field allows the outflow momenta to be deposited more efficiently inside the clump. Thus, the massive star formation in the simulated turbulent, magnetized, parsec-scale clump

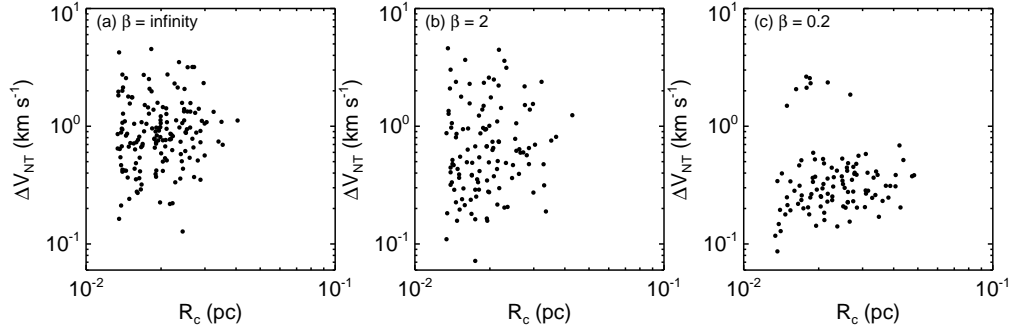


**FIGURE 3.** Nonthermal 3D velocity dispersions as a function of core radii for three models with different magnetic field strengths: (a) model N1 (no magnetized), (b) model W1 (weakly magnetized), and (c) model S1 (strongly magnetized). The sound speed is  $c_s = 0.266 \text{ km s}^{-1}$ , corresponding to  $T = 20 \text{ K}$ . See Nakamura & Li (2011) in more detail.

is outflow-regulated and clump-fed. An important implication is that the formation of low-mass stars in a dense clump can affect the formation of massive stars in the same clump, through their outflow feedback on the clump dynamics.

In addition, contrary to the common expectation, a magnetic field of the strength in the observed range decreases, rather than increases, the characteristic stellar mass. It (1) reduces the number of intermediate-mass stars that are formed through direct turbulent compression, because sub-regions of the clump with masses comparable to those of stars are typically magnetically subcritical and cannot be compressed directly into collapse, and (2) increases the number of low-mass stars that are produced from the fragmentation of dense filaments. The filaments result from mass accumulation along the field lines. In order to become magnetically supercritical and fragment, the filament must accumulate a large enough column density (proportional to the field strength), which yields a high volume density (and thus a small thermal Jeans mass) that is conducive to forming low-mass stars. The characteristic stellar mass is reduced further by outflow feedback. The conclusion is that both magnetic fields and outflow feedback are important in shaping the stellar initial mass function (see Figure 2).

## Physical Properties of Dense Cores in Cluster Formation

In the outflow-regulated cluster formation model, the physical properties of dense cores in cluster-forming clumps are also different from those in quiescent star-forming regions like Taurus. Nakamura & Li (2011) have performed a set of 3D MHD simulations of cluster formation taking into account the effects of protostellar outflow feedback and identified dense cores by applying a clumpfind algorithm to the simulated 3D density data cubes. The main results are summarized as follows. (1) The velocity dispersions of dense cores show little correlation with core radius, irrespective of the strength of the magnetic field and outflow feedback (see Figure 3). In the absence of a magnetic field, the majority of the cores have supersonic velocity dispersions, whereas in the presence of a moderately strong magnetic field, the cores tend to be subsonic or at most transonic.

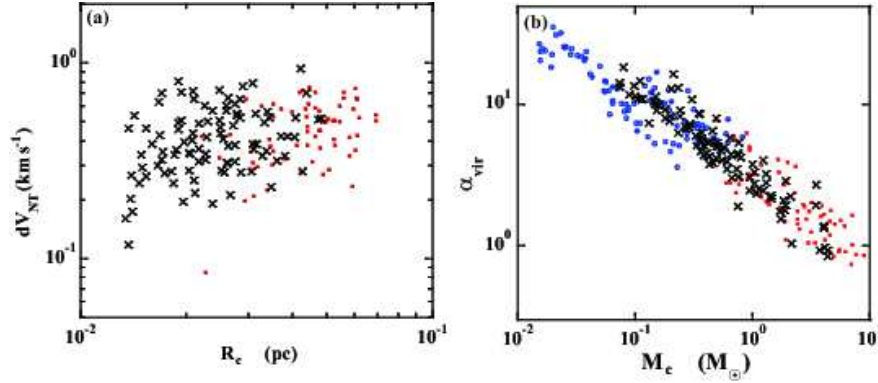


**FIGURE 4.** The relationship between the 1D FWHM nonthermal velocity width and core radius for the dense cores in the  $\rho$  Ophiuchi Main Cloud and our cores identified from the moderately strong magnetic field model (model S1). The red dots and black crosses denote the  $\rho$  Oph cores and our cores of model S1, respectively. For the  $\rho$  Oph cores, we used the results of Maruta et al. (2010) who identified the cores using  $\text{H}^{13}\text{CO}^+$  ( $J = 1 - 0$ ) data. (b) The virial-parameter-core-mass relation. The red dots and black crosses are the same as those of panel (a). The blue open circles denote the cores of NGC 1333 identified using  $\text{N}_2\text{H}^+$  ( $J = 1 - 0$ ) emission (Walsh et al. 2007). See Nakamura & Li (2011) in more detail.

(2) Most of the cores are out of virial equilibrium, with the external pressure due to ambient turbulence dominating the self-gravity. The core formation and evolution is largely controlled by the dynamical compression due to outflow-driven turbulence. Such a situation is in contrast to the strongly magnetized (magnetically subcritical) case, where the self-gravity plays a more important role in the core dynamics, particularly for massive cores (Nakamura & Li 2008). (3) Even an initially weak magnetic field can retard star formation significantly, because the field is amplified by supersonic turbulence to an equipartition strength. In such an initially weak field, the distorted field component dominates the uniform one. In contrast, for a moderately strong field, the uniform component remains dominant. Such a difference in the magnetic structure can be observed in simulated polarization maps of dust thermal emission. Recent polarization measurements show that the field lines in nearby cluster-forming clumps are spatially well ordered, indicative of a moderately strong, dynamically important, field (see Figure 5b, e.g., Sugitani et al. 2010, 2011).

The characteristics of dense cores formed in dense clumps with moderately strong magnetic fields are in good agreement with observations of  $\rho$  Oph, the nearest cluster-forming clump (Maruta et al. 2010), where subsonic or transonic internal motions are observed in dense cores, most of which appear gravitationally-unbound or pressure-confined (see Figure 4).

## COMPARISON WITH OBSERVATIONS

Recently, several extensive molecular outflow surveys towards cluster forming regions have been done using the molecular outflow tracers, CO lines. Here, we summarize the survey results toward 5 nearby cluster-forming clumps. Since all 5 regions contain no massive stars emitting strong UV, the outflow feedback is expected to be the leading

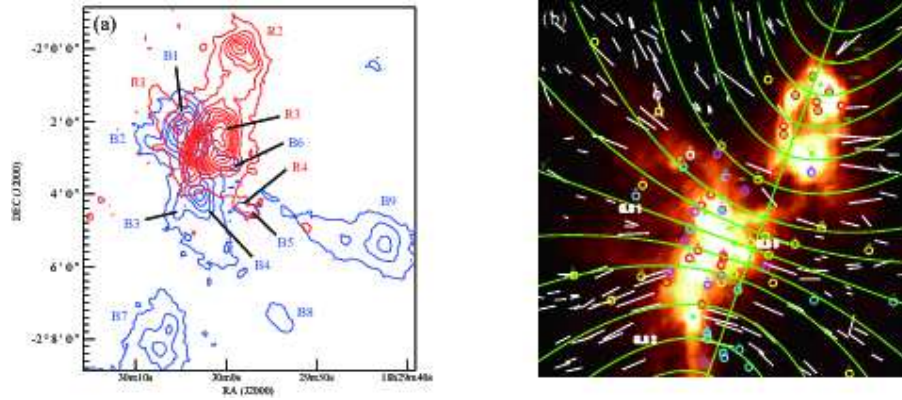


**FIGURE 5.** (a) Molecular outflow lobes identified from CO ( $J = 3 - 2$ ) emission toward the Serpens South protocluster. The blue contours represent blueshifted  $^{12}\text{CO}$  gas and red contours represent redshifted  $^{12}\text{CO}$  gas. The blue and red contour levels go up in  $6 \text{ K km s}^{-1}$  steps, starting from  $3 \text{ K km s}^{-1}$ . The integration ranges are  $-9.75$  to  $3.75 \text{ km s}^{-1}$  for blueshifted gas and  $11.25$  to  $29.25 \text{ km s}^{-1}$  for redshifted gas. See Nakamura et al. (2011b) in more detail. (b) H-band polarization vectors (white lines) toward the Serpens Main cloud, and their best-fit magnetic field (green thick curved/straight lines and thin curved lines), superposed on SCUBA  $850 \mu\text{m}$  continuum image. The horizontal axis (green thin straight line), which is perpendicular to the parabolic magnetic field axis (green thick straight line), is also shown. YSOs identified by the Spitzer Space Telescope are marked by circles (Class 0/I; red, Flat spectrum; magenta, Class II; yellow, Transition disk; blue, Class III; white) with ID numbers (Tables 3 and 4 of Winston et al. 2007). Submillimeter continuum peaks are shown by crosses with names and their coordinates come from the Spitzer photometry of Winston et al. (2007), except SMM2 and SMM11 (Davis et al. 1999).

stellar feedback mechanism. An example of these outflow surveys is shown in Figure 5, where blueshifted and redshifted CO ( $J = 3 - 2$ ) integrated intensity contours are indicated towards the nearest cluster-forming, infrared dark cloud, Serpens South ( $d \sim 400 \text{ pc}$ ). Several molecular outflow lobes are crowded in the central dense region where about 100 YSOs are located and forming a protocluster. The overlapping outflow structure is a common characteristic of active cluster forming clumps, suggesting that the outflows influence the structure formation in the clumps significantly.

Table 1 summarizes some physical properties of the outflows for the 5 regions. From the observational data, we can now address the two important issues of the cluster formation: turbulent generation and clump destruction. If we compare between the turbulent dissipation rate and outflow energy injection rate, we can verify whether the outflow feedback can maintain the supersonic turbulence in the clumps. As for the clump destruction, we can compare the global gravitational force and the force exerted by the outflows. The outflow force must be comparable to the clump gravitational force if the outflow feedback plays an important role in the clump destruction.

According to Table 1, for all the clumps, the outflow energy injection rate is comparable to or larger than the turbulence dissipation rate. So, we conclude that the outflows can maintain supersonic turbulence in the cluster-forming clumps. On the other hand, how the outflow force impacts the global clump dynamics appears to depend on the clump mass. For the clumps with masses larger than about  $400 M_{\odot}$ , the clump gravitational force tends to be significantly larger than the outflow force, whereas for the clumps with masses smaller than about  $400 M_{\odot}$ , the outflow force is comparable to the clump gravi-

**TABLE 1.** Observations of nearby parsec-scale cluster-forming clumps

Name	Mass ( $M_{\odot}$ )	$\dot{E}_{\text{turb}}$ ( $L_{\odot}$ )	$\dot{E}_{\text{out}}$ ( $L_{\odot}$ )	$\dot{E}_{\text{out}}/\dot{E}_{\text{turb}}$	$F_{\text{grav}}$ ( $M_{\odot}$ km/s)	$F_{\text{out}}$ ( $M_{\odot}$ km/s)	$F_{\text{out}}/F_{\text{grav}}$	Ref.*
L1641N	200	0.1	2	20	6	10	1.7	1
Serpens Main	400	0.2	1	10	2	5	2.5	2
Serpens South	500	0.2	1	5	40	8	0.2	3
rho Oph	1000	0.1	0.2	2	13	1	0.08	4
NGC 1333	2000	0.5	0.7	1.4	20	6	0.3	5

\* 1: Nakamura et al. (2012), 2: Graves et al. (2010), 3: Nakamura et al. (2011b), 4: Nakamura et al. (2011a), 5: Arce et al. (2010)

tational force. It may be difficult to destroy the whole clumps only by the outflow feedback for the clumps with masses larger than  $400 M_{\odot}$ . In contrast, the current observed outflow activity can destroy the small clumps or at least change the clump dynamics significantly. Since the typical YSO ages are around a few Myr, the cluster formation may last for several or more free-fall times. That supports the slow cluster formation scenario or the outflow-regulated cluster formation scenario. However, the importance of the outflow feedback in cluster formation may depend on the clump mass and therefore further detailed investigation will be needed to uncover the role of protostellar outflow feedback in cluster formation.

## REFERENCES

1. Arce, H. G., Borkin, M. A., Goodman, A. A., Pineda, J. E., & Halle, M. W. 2010, *ApJ*, 715, 1170
2. Carroll, J. J., Frank, A., Blackman, E. G., et al. 2009, *ApJ*, 695, 1376
3. Davis, C. J., et al. 1999, *MNRAS*, 309, 141
4. Graves, S. F., et al. 2010, *MNRAS*, 409, 1412
5. Lada, C. J., & Lada, E. A. 2003, *ARA&A*, 41, 57
6. Li, Z.-Y., & Nakamura, F. 2006, *ApJ*, 640, L187
7. Li, Z.-Y., Wang, P., Abel, T., & Nakamura, F. 2010, *ApJ*, 720, L26
8. Higuchi, A. E., Kuroono, Y., Saito, M., & Kawabe, R. 2009, *ApJ*, 705, 468
9. Maruta, H., Nakamura, F., Nishi, R., Ikeda, N., & Kitamura, Y. 2010, *ApJ*, 714, 680
10. Matzner, C. D., & McKee, C. F. 2000, *ApJ*, 545, 364
11. Matzner, C. D. 2007, *ApJ*, 659, 1394
12. Nakamura, F., & Li, Z.-Y. 2007, *ApJ*, 662, 395
13. Nakamura, F., & Li, Z.-Y. 2008, *ApJ*, 687, 354
14. Nakamura, F., & Li, Z.-Y. 2011, *ApJ*, 740, 36
15. Nakamura, F., Kamada, Y., Kamazaki, T., et al. 2011a, *ApJ*, 726, 46
16. Nakamura, F., Sugitani, K., Shimajiri, Y., et al. 2011b, *ApJ*, 737, 56
17. Nakamura, F., Miura, T., Kitamura, Y. et al., 2012, *ApJ*, 746, 25
18. Rathborne, J. M., Jackson, J. M., & Simon, R. 2006, *A&A*, 641, 389
19. Ridge, N. A., Wilson, T. L., Megeath, S. T., Allen, L. E., & Myers, P. C. 2003, *AJ*, 126, 286
20. Smith, R. J., Longmore, S., Bonnell, I. 2009, *MNRAS*, 400, 1775
21. Sugitani, K., Nakamura, F., Tamura, M., et al. 2010, *ApJ*, 716, 299
22. Sugitani, K., Nakamura, F., Watanabe, M., et al. 2011, *ApJ*, 734, 63
23. Walsh, A. J., Myers, P. C., Di Francesco, J., et al. 2007, *ApJ*, 655, 958
24. Wang, P., Li, Z.-Y., Abel, T., & Nakamura, F. 2010, *ApJ*, 709, 27
25. Winston, E., et al. 2007, *ApJ*, 669, 493